Journal of Materials Chemistry B

ROYAL SOCIETY OF CHEMISTRY

PAPER

View Article Online
View Journal | View Issue

Cite this: J. Mater. Chem. B, 2022, 10, 6655

An artificial antibody for exosome capture by dull template imprinting technology†

Lukuan Liu,‡[ab] Jianhui Liu,‡[a] Wen Zhou,[ac] Zhigang Sui,[a] Jing Liu,[b] Kaiguang Yang,*[a] Lihua Zhang,*[a] Zhen Liang[a] and Yukui Zhang[a]

Received 7th March 2022,
Accepted 20th April 2022

DOI: 10.1039/d2tb00494a

rsc.li/materials-b

Exosomes are extracellular vesicles with unique size distribution derived from the parent cells. They are involved in intercellular communication and transport, and are also biomarkers for early diagnosis and prognosis of disease. However, the isolation and characterization of exosomes face the challenges of large sample requirements and low enrichment efficiency of traditional methods. Herein, a simple method is proposed for the preparation of an artificial antibody that has a synergistic effect by featuring nanocavities obtained by dull template imprinting and molecular recognition conferred by electrostatic interaction. With this artificial antibody, highly efficient capture and proteome analysis of exosomes from urine and cell culture media are achieved: for urine, the abundance of Top100 exosomal proteins enriched by this artificial antibody increased from 1.85% to 9.66%. For the cell culture medium, the abundance of the Top100 proteins enriched by this artificial antibody was 28.4%. Moreover, this artificial antibody has a comparable effect to the commercial precipitation-based method in capturing exosomes and has advantages in removing contaminants such as prothymosin alpha (PTMA), demonstrating the superior selectivity of the artificial antibody. Overall, this artificial antibody holds promise to capture exosomes from biofluids and is compatible with subsequent proteome analysis.

Introduction

Exosomes are small extracellular vesicles with a diameter between 40 and 160 nm secreted by most cells. They are widely found in cell culture media, blood, urine and other biofluids.[1] Exosomes carry important functional components such as nucleic acids, lipids, metabolites and proteins from parent cells.[2] Among them, proteins in exosomes mediate material transport and information exchange between cells, and participate in many physiological and pathological processes such as regulation of cell proliferation and migration, antigen presentation, immune response, and tumor development.[3–6] However, biofluids in which exosomes are presented are complex and have many interfering components such as non-exosomal vesicles, apoptotic bodies, protein aggregates, chylomicrons and lipoprotein particles.[7] Moreover, the abundance of exosomes is extremely low. For example, the number of extracellular vesicles in platelet-free plasma only accounts for 0.0035% of the total number of particles in plasma. The content of exosomal vesicles is lower and contains only 1 μg protein per 3×10^{10} vesicles.[8,9] Therefore, enriching exosomes with high efficiency and selectivity is an important prerequisite for their proteomic research.

To date, many techniques for capturing exosomes from biofluids have been developed using the physicochemical and biochemical properties of exosomes.[10–14] Among them, ultracentrifugation technology is currently the most widely used method.[15] However, this technique requires large amounts of samples, and the recovery rate of exosomes is low, so it cannot be used for exosome isolation and analysis of trace and precious samples. Therefore, researchers developed an exosome isolation method based on the principle of polyethylene glycol (PEG) precipitation.[16] Compared to ultracentrifugation, the PEG precipitation technique requires lower sample volumes and achieves higher recovery rates. However, this technique suffers from co-precipitation of other non-exosomal contaminants, such as lipoproteins, leading to a low purity of exosomes. Other exosome isolation techniques, such as size exclusion, dialysis, immunomagnetic beads, microfluidics, and aptamer-based and lipid-based methods, often include complex processes, low throughput, and large sample requirements, and the purity has not been significantly improved.[10,17–19] Therefore, it is still necessary to develop a novel and efficient exosome capture method for proteomic analysis.

[a] CAS Key Laboratory of Separation Sciences for Analytical Chemistry, Dalian Institute of Chemical Physics, Chinese Academy of Sciences, Dalian 116023, China. E-mail: yangkaiguang@dicp.ac.cn, lihuazhang@dicp.ac.cn
[b] Stem Cell Clinical Research Center, The First Affiliated Hospital of Dalian Medical University, Dalian 116011, China
[c] University of Chinese Academy of Sciences, Beijing, 100049, China

† Electronic supplementary information (ESI) available. See DOI: https://doi.org/10.1039/d2tb00494a

‡ These authors contributed equally to this work.

As a novel artificial antibody preparation technique that combines shape matching and chemical recognition, molecular imprinting can be used to recognize target molecules independent of antibodies and is more versatile and easier to tailor.[20] Our previous work has shown that molecular imprinting has been successfully used to capture tumor cells by using fixed cells as templates.[20–22] Conceivably, by using exosomes as templates, molecular imprinting could provide nanocavities that precisely match the shape and chemical properties of the exosomes. These nanocavities could act as antibodies to capture exosomes from biofluids. However, it is difficult to obtain adequate and pure exosomes to be used as templates due to the limitation of current exosome capture methods. Therefore, we speculate that it may be a good choice to prepare artificial antibodies for exosome capture by synthesizing nanoparticles with similar size distribution and surface properties to exosomes as dull templates.

It has been proven that the exosome membrane is negatively charged and can interact with positively charged molecules. The anion exchange resin was successfully used to capture exosomes.[23] However, this method requires collection of different effluent fractions, and contaminants and exosomes may co-elute, thus reducing the recovery rate and purity. Predictably, the use of electrostatic interaction is expected to provide further enhancement of exosome-specific capture sensitivity when the cationic molecules are integrated into the molecular imprinting process.

In this paper, an artificial antibody (molecule imprinting polymer, MIP) for exosome capture was constructed based on dull template imprinting and electrostatic interaction. The MIP possesses nanocavities that precisely match the shape and molecular binding features of the target exosomes. By the synergistic effect of conformational recognition and electrostatic interaction, the MIP has been used to capture exosomes from urine and cell conditioned media. The enrichment effect of the MIP on exosomes was further evaluated at the protein level by using a quantitative proteomic method and Gene Ontology analysis.

Experimental

Materials

Methanol was purchased from Thermo Fisher (PA, USA). Trypsin, ammonia solution (28%), tetraethyl orthosilicate (TEOS, 98%), methylenebisacrylamide (MBA), acrylamide (AAm), 2-(diethylamino)ethyl acrylate, sodium dodecyl sulfonate (SDS), azodiisobutylamidine hydrochloride (AIBA), dithiothreitol (DTT), urea, iodoacetamide (IAA) and ammonium bicarbonate (ABC) were purchased from Sigma-Aldrich (MO, USA). Hydrofluoric acid was purchased from Tianjin Kemiou Chemical Reagent Co., Ltd (Tianjin, China). The TEI kit was purchased from Thermo Fisher (CA, USA). Ultrafiltration centrifuge tubes (10 kDa) were purchased from Sartorius (Goettingen, Germany). The deionized water used in the experiments was purified using a Milli-Q system (MA, USA).

Cell culture and pre-treatment of the cell culture medium

HeLa cells were cultured for at least six passages using stable isotope labeling with amino acids in cell culture (SILAC) (Lys6, Arg10). When the cells grew to 80–90% confluence, the SILAC-labeled medium containing fetal bovine serum (exosomes removed) was collected. The obtained culture medium was centrifuged successively to remove cells (500*g*) and cell debris (3000*g*). The supernatant was collected and filtered with a 0.22 μm sterile filter to obtain the HeLa-CCM for exosome capture.

Preparation of silica nanoparticles

50 mL of methanol, 7.74 mL of water, and 5 mL of 28% ammonia water were mixed, and then 1.90 mL of TEOS was added rapidly. The solution was stirred at 40 °C for 30 min and then centrifuged at 6000*g* to obtain silica nanoparticles. Finally, the silica nanoparticles were washed three times with water and dispersed in 1 mL of water to use them as dull templates. The particle size distribution and ζ-potential in the aqueous solution were measured by dynamic light scattering using a Nano-ZS90 particle sizer (Malvern, UK).

Preparation of the artificial antibody for exosome capture by the dull template method

0.50 g of MBA, 0.01 g of AAm, 0.01 g of 2-(diethylamino)ethyl acrylate and 100 μL of silica nanoparticle solution were dissolved and dispersed into 6 mL of water. Then, 0.03 g of AIBA was added to initiate polymerization at 60 °C for 24 h. After that, the polymer was dried and the silica nanoparticles were etched by using hydrofluoric acid. Finally, the polymer was washed with water three times and dried to obtain the artificial antibody (MIP). The morphology of the MIP was characterized using a JSM-7800F scanning electron microscope.

Capture of exosomes from urine and HeLa-CCM using the MIP

The MIP dispersed in methanol was loaded into pipette tips (200 μL) and then centrifuged (10 000*g*) for 10 min until the height of the MIP in the pipette tips reached about 1 cm. Then the pipette tips were washed three times with water for capturing exosomes from urine and HeLa-CCM. 1 mL of urine or 3 mL of HeLa-CCM was loaded into the above pipette tips and centrifuged (16 000*g*) for 20 min. The MIP was aspirated by using 4% SDS solution and then centrifuged at 16 000*g* for 10 min. The supernatant was obtained for later usage. A PEG-based commercial TEI kit (KIT) was used as the control and processed according to the instructions.

Proteomic analysis of MIP-isolated exosomes from urine and HeLa-CCM by mass spectrometry

In this paper, the filter-assisted sample pretreatment method (FASP) was used to prepare peptides for mass spectrometry (MS) analysis. The above supernatants were reduced with 100 mM DTT at 95 °C for 10 min and diluted with 8 M urea. Then the diluted samples were loaded in the filter unit and centrifuged at 14 000*g* for 15 min. Then the proteins were alkylated with 50 mM IAA at room temperature in the dark

and then rinsed with urea and ammonium bicarbonate successively. Then the proteins were digested with trypsin at 37 °C for 18 h. The tryptic peptides were collected through centrifugation.

The tryptic peptides were vacuum-dried and analyzed on an Orbitrap Fusion Lumos Tribrid mass spectrometer (Thermo Scientific, USA) coupled with an EASY-nLC 1200 (Thermo Scientific, USA). The injected digest was separated on a reverse phase (RP) C18 analytical column (14 cm × 150 μm i.d.) at a flow rate of 600 nL min^{-1}. The separation gradient was employed as follows: from 4% to 25% buffer B (80% ACN/0.1% FA) for 61 min, from 25% to 50% buffer B for 10 min, from 50% to 95% buffer B for 1 min, and from 95% to 95% buffer B for 3 min. The mass spectrometry data were acquired in the data dependent mode. The scan range for full scan was set from 350 *m*/*z* to 1500 *m*/*z* in the Orbitrap with a resolution of 60 000 (at 200 *m*/*z*). The AGC target was set as 4×10^5, and the maximum injection time was set as 50 ms. Within the cycle time of 3 s, ions were sequentially isolated with a 1.6 *m*/*z* isolation window and fragmented by HCD with a collision energy of 30%. The tandem mass spectra were obtained using Orbitrap (resolution: 15 000 at 200 *m*/*z*) with the AGC target set at 5×10^4 and the maximum injection time at 30 ms.

The obtained raw data were searched using MaxQuant (v1.6.17.0) against the Swiss-Prot human protein database (UniProt Proteome, release 2022_02, 42 358 entries). Fully tryptic cleavage constraints were set with up to two cleavage sites. Cysteine carbamidomethylation (+57.0215 Da) was set as fixed modification. Methionine oxidation (+15.9949 Da) and protein N-terminal acetylation (+42.0106 Da) were set as variable modifications. For HeLa cell culture medium samples, SILAC-labeled lysine and arginine (Lys6, Arg10) were added as variable modifications. The mass tolerances were 10 ppm for the full scan and 20 ppm for the tandem mass spectra. The intensity-based absolute quantification (iBAQ) approach was used to calculate protein abundances. The intensity-based fraction of total (iFOT) was used to represent the normalized abundance of a protein across experiments.[24] The option 'match between runs' was enabled with a 1 min time window. Gene Ontology (GO) term enrichment analysis and protein–protein network analysis were based on DAVID 2021 (Dec. 2021) and STRING (version 11.5) databases.

Results and discussion

Preparation and characterization of the MIP

To achieve highly selective capture of exosomes, we developed an artificial antibody (MIP) with electrostatic and steric synergistic effects for exosome capture by dull template imprinting (Fig. 1).

Molecularly imprinted materials mainly use the imprinted sites left by templates to recognize target molecules, but the premise of conventional preparation methods is to use target molecules with high purity as templates. Due to the limitation of exosome capture methods, all the currently obtained exosomes contain non-vesicular contaminants such as lipoproteins and protein aggregates to a certain extent. If the currently available exosomes are directly used as templates, the imprinted sites from contaminants will inevitably be introduced, resulting in the inability to improve the capture specificity of exosomes substantially.

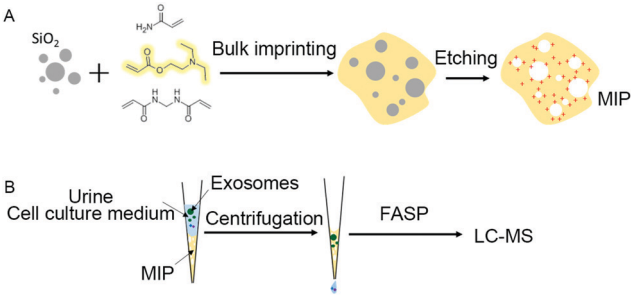

Fig. 1 Preparation of the artificial antibody (MIP) by using silica templates (A) and the MIP tips fabricated for capturing exosomes in urine and the cell culture medium (B).

Therefore, in order to capture exosomes specifically, we synthesized silica nanoparticles as dull templates with similar size distribution properties to exosomes, and the distribution range is between 40 nm and 160 nm (Fig. 2A). The silica nanoparticles in the aqueous solution were negatively charged, which was similar to exosomes, and the ζ-potential was about −39.6 mV (Fig. 2B).[25] Then, the cationic functional monomer 2-(diethylamino)ethyl acrylate was introduced during the polymerization process to form an electrostatic adsorption effect for the negatively charged exosome membrane. Moreover, the hydrophilic monomer acrylamide and the hydrophilic cross-linker *N*,*N*′-methylene diacrylamide were used as the imprinting system to reduce nonspecific adsorption and improve biocompatibility. After polymerization and template removal, imprinted sites similar in size to exosomes were left inside the

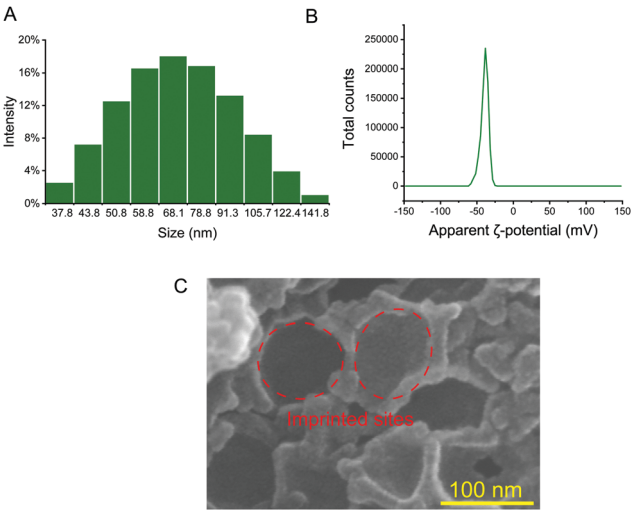

Fig. 2 Size distribution of silica nanoparticles (A); ζ-potential of silica nanoparticles in aqueous solution (B); and scanning electron micrograph of the MIP (C).

MIP (Fig. 2C). As shown in Fig. 1B, the synthesized MIP was packed into pipette tips to capture exosomes in complex samples and the captured particles were further used for proteome and GO analysis to determine whether these particles contain proteins, which are representative of exosomes.

Nanoparticle tracking analysis (NTA) of MIP-isolated exosomes from urine and HeLa-CCM

We analyzed the size distribution of particles isolated by the MIP from urine and HeLa-CCM by performing NTA. As shown in Fig. S1 (ESI†), for experiments that used urine as a source of exosomes, particles isolated by the MIP have a concentration of 1.30×10^{10} particles per mL. For experiments that used HeLa-CCM as a source of exosomes, particles isolated by the MIP have a concentration of 2.70×10^{9} particles per mL. These results also demonstrate that the MIP is able to isolate particles within the size range of exosomes from human urine and HeLa-CCM.

Proteomic analyses of MIP-isolated exosomes from urine

The number of quantified proteins. Proteins were extracted from MIP-isolated exosomes and analyzed by LC-MS in triplicate. Untreated urine and the PEG-based commercial kit (KIT) were treated as controls. As shown in Fig. 3A, over 1200 proteins were quantified in three MS replicates from MIP-isolated exosomes with good reproducibility ($R^2 \geq 0.95$, Fig. 3B), comparable to the reproducibility of untreated urine and KIT-isolated exosomes (Fig. S2, ESI†). By combining the proteome results from three replicates, the total numbers of proteins quantified from untreated urine, KIT-isolated and MIP-isolated exosomes were 1359, 1583 and 1395, respectively (Fig. 3C). A total of 1326 proteins from MIP-isolated exosomes were found in common with the proteins quantified in the KIT-isolated exosomes, representing 95.05% of the proteins identified in the MIP-isolated exosomes. These results indicate that the majority of proteins found in the MIP-isolated exosomes from urine are also found in KIT-isolated exosomes.

Enrichment effect analysis of MIP-isolated exosomes based on Top100 proteins and exclusion markers in datasets of extracellular vesicles. As shown in Fig. 4A, the frequently used exosomal biomarkers, including CD9, CD63, CD81, FLOT-1, HSP90AA1, HSP90AB1 and TSG101, were abundant in both the MIP-isolated and KIT-isolated exosomes.[26] Notably, due to the high resolution and sensitivity of mass spectrometry, these marker proteins, except for FLOT-1, were also quantified in untreated urine. Therefore, the way to determine the purity of exosomes using only marker proteins needs to be improved, because this method will overestimate the purity of exosomes. Top100 proteins refer to about 100 proteins that are most frequently identified in exosome enrichment studies and are also one of the most reliable datasets to identify the source of exosomes. The qualitative and quantitative information of these marker proteins obtained using a high-resolution MS-based proteomics technique can be an effective complement to current methods to determine exosome purity in a large scale. In this study, 125 proteins were collected as Top100 proteins by combining the Top100 proteins from both ExoCarta and Vesiclepedia datasets.[27,28] The results showed that 77.5% (97/125) of the Top100 proteins were found in the untreated urine. After enrichment by the MIP, 88.8% (111/125) of the Top100 proteins were identified. In contrast, the percentage of the Top100 proteins is also 88.8% (111/125) after KIT capture.

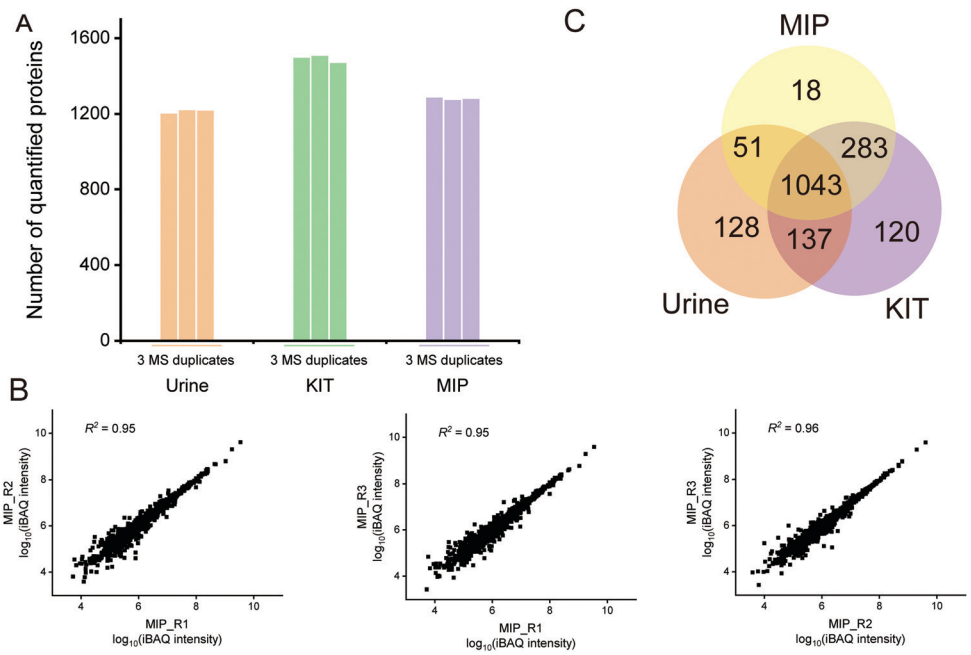

Fig. 3 The number and reproducibility of quantified exosome proteins from urine isolated by the MIP. (A) The quantified protein numbers from untreated urine, KIT-isolated and MIP-isolated exosomes. (B) The quantified reproducibility among three MS replicates for the proteins from the MIP-isolated exosomes. (C) The Venn diagram of proteins quantified from untreated urine, KIT-isolated and MIP-isolated exosomes.

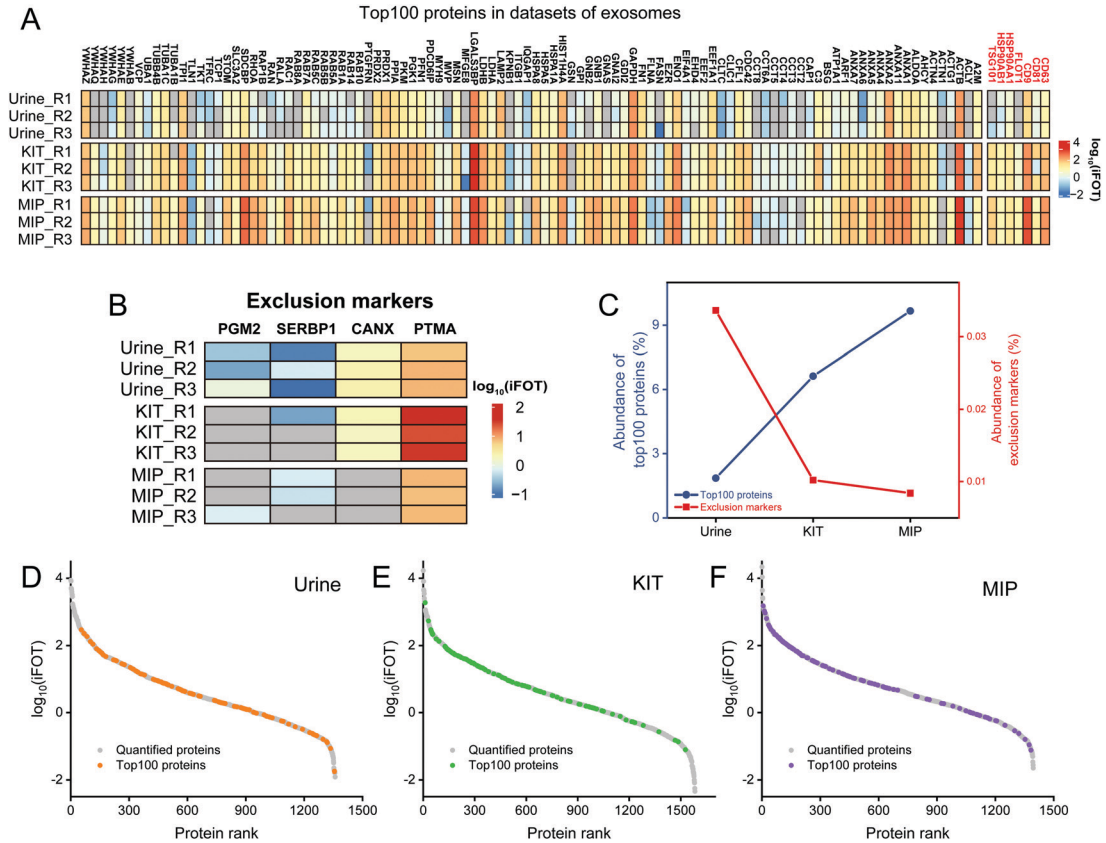

Fig. 4 Enrichment effect analysis of MIP-isolated exosomes based on Top100 proteins and exclusion markers in datasets of extracellular vesicles. (A) Heatmap of Top100 protein intensities in untreated urine, KIT-isolated and MIP-isolated exosomes. The frequently used exosomal biomarkers are marked in red. (B) Heatmap of exosomal exclusion marker intensities in the three samples. (C) The relative abundance of Top100 proteins and exclusion markers in the three samples. Ranking of quantified proteins based on iBAQ intensities in untreated urine (D), KIT-isolated exosome (E) and MIP-isolated exosome (F) samples. The Top100 proteins are separately marked in orange (D), green (E) and purple (F).

In addition to the enrichment of Top100 proteins, the removal of contaminants is also an important indicator for evaluating the enrichment effect of exosomes. The frequently used exclusion markers such as HMGB1, CANX, EIF4B, COX5B, PDAP1, HMGB2, SKP1, EIF4H, MAPRE1, PGM2, PTMA, HMGB3, SERBP1 and SLIRP were also studied.[26] As shown in Fig. 4B, both SERBP1 and PTMA were present in untreated urine, KIT-isolated and MIP-isolated exosomes, which needed to be removed by developing new methods. The abundances of PGM2, SERBP1 and CANX were decreased and not even quantified after enrichment by the MIP and KIT. Notably, the abundance of PTMA in KIT-isolated exosomes was significantly higher than that in MIP-isolated exosomes. Qualitatively, these results indicate that the MIP has a comparable effect to the PEG-based method in capturing exosomes and has advantages in removing contaminants, such as PTMA.

Furthermore, in order to evaluate the purity of exosomes with the information of protein abundance, the quantitative information of exosome marker proteins and exclusion markers was also analyzed. As shown in Fig. 4C, iBAQ quantitative analysis of the identified proteins showed that the abundance of the Top100 proteins identified in untreated urine was only 1.85%, which was mainly due to the fact that the majority of the high abundance proteins in urine were not exosome-derived proteins. After the enrichment of the commercialized KIT, the abundance of the Top100 proteins increased to 6.62%. In contrast, after the enrichment of the MIP, the abundance of the Top100 proteins increased to 9.66%, and the abundance of exclusion markers decreased to 0.0084%, indicating that electrostatic interactions and steric effects can significantly increase the abundance of the exosome-derived proteins.

In order to investigate the protein composition of exosomes and the abundance distribution of Top100 proteins, we ranked the identified proteins using the intensity information obtained by the iBAQ quantitative method. The exosome proteins were averagely divided into three categories by their abundance and we define the most abundant range as high-abundance proteins. For the Top100 proteins from urine, KIT-isolated and MIP-isolated exosomes, the numbers in the high-abundance protein range were 29, 66 and 65, respectively (Fig. 4D–F). The significantly increased abundance of Top100 proteins indicated that the MIP has a good effect in increasing the abundance of exosome-derived proteins.

GO analysis of MIP-isolated exosomes based on the databases of extracellular vesicles. To confirm that the proteins identified in the MIP-isolated exosomes were *bona fide*

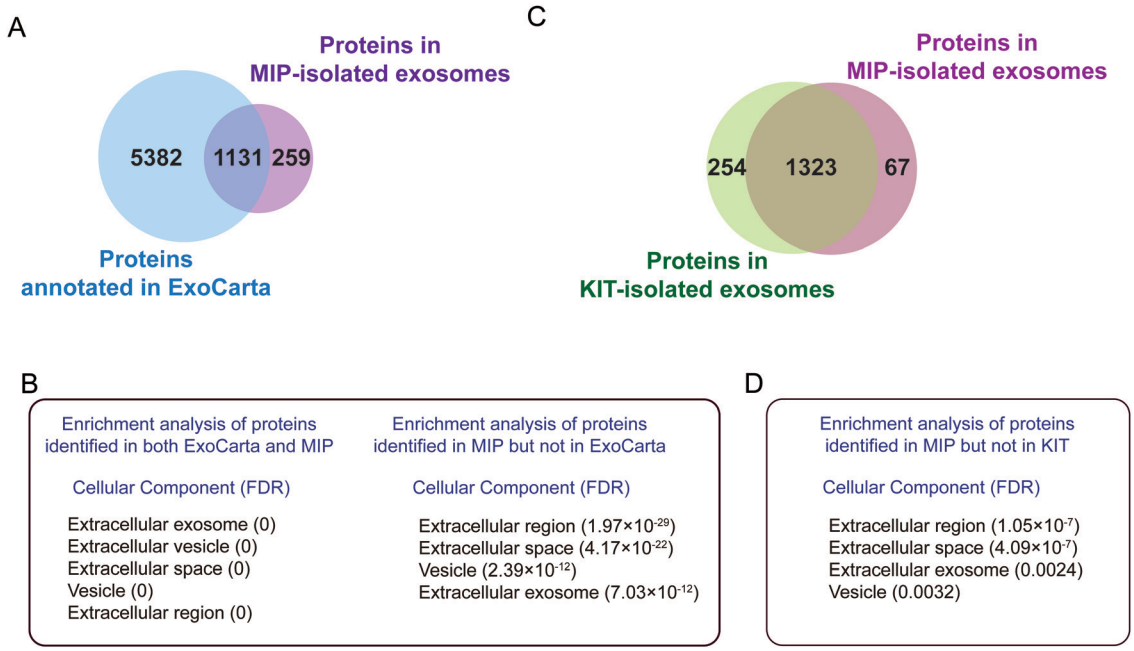

Fig. 5 GO analysis of MIP-isolated exosomes based on the databases of extracellular vesicles. (A) The Venn diagram of exosome proteins isolated by the MIP compared with proteins annotated in ExoCarta. (B) GO enrichment analysis for the cell components of proteins identified in both ExoCarta and the MIP (left) and in the MIP but not in ExoCarta (right). (C) The Venn diagram of exosome proteins isolated by the MIP and KIT. (D) GO enrichment analysis for the cell components of proteins identified in the MIP but not in KIT.

exosome-associated proteins, we compared the proteomic data of our MIP-isolated exosomes with the human protein data annotated in the ExoCarta database, followed by the GO analysis. As shown in Fig. 5A, 81.4% of the proteins in the MIP-isolated exosomes matched the human proteins annotated in the ExoCarta database. Protein–protein interaction (PPI) analysis of the subset of 1131 proteins quantified in both MIP-isolated exosomes and the ExoCarta database revealed a highly interconnected network (Fig. S3A, ESI†). Prominent GO categories of the 1131 proteins were related to extracellular exosomes, extracellular vesicles and the extracellular space (Fig. 5B). Prominent GO categories of the 259 proteins identified in MIP-isolated exosomes but not in the ExoCarta database were also related to the extracellular region, extracellular space and extracellular exosomes. These proteins participated in biological processes such as cell adhesion and immune response (Table S1, ESI†). The protein list obtained from MIP-isolated exosomes has the potential to serve as an effective complement to protein data in the ExoCarta database.

We further comparatively analyzed the proteomes of KIT-isolated and MIP-isolated exosomes. 95.2% of the proteins in the MIP-isolated exosomes were also found in the KIT-isolated exosomes (Fig. 5C). Prominent GO categories of the 67 proteins identified in MIP-isolated exosomes but not in KIT-isolated exosomes were also related to the extracellular region, extracellular space and extracellular exosomes (Fig. 5D). These results further support the conclusion that the MIP can isolate exosomes effectively from urine. The above results show that, in urine samples, from the protein level, the MIP can not only increase the enrichment abundance of exosome marker proteins, but also increase the proportion of proteins localized in exosomes.

Proteomic analyses of MIP-isolated exosomes from HeLa-CCM

In view of the excellent enrichment ability of the MIP for exosomes in urine, we further introduced the MIP to the enrichment of exosomes in HeLa-CCM. The enrichment ability of the MIP to selectively capture exosomes in HeLa-CCM was evaluated by qualitative and quantitative proteome analysis of exosomes derived from the SILAC-labeled HeLa cells. Protein samples from MIP-isolated exosomes in HeLa-CCM were analyzed in triplicate. As shown in Fig. 6A, over 450 proteins were quantified in three MS replicates from MIP-isolated exosomes with good reproducibility ($R^2 \geq 0.87$, Fig. 6B–D). Exosomes are derived from labeled cells, so the ratio of the labeled proteins determines the enrichment ability of the MIP. In this study, the labeled proteins accounted for more than 89.5% of the total identified proteins, indicating that the MIP has a significant effect in removing non-cellular contaminants.

To further analyze the enrichment effect of MIP-isolated exosomes from HeLa-CCM, the expression profiles of the Top100 proteins and exclusion markers in datasets of extracellular vesicles are depicted in Fig. 7A and B. The results showed that 72% (90/125) of the Top100 proteins including the commonly used exosome markers such as CD9, CD81, HSP90AA1 and HSP90AB1 were found in the MIP-isolated exosomes from HeLa-CCM, and the abundance of the Top100 proteins was 28.4%. Among them, 52.2% (47/90) of the Top100 proteins were highly abundant (Fig. 7C). The exclusion markers such as HMGB1, EIF4B, SERBP1, CANX and NOLC1 were identified in the MIP-isolated exosomes from HeLa-CCM, but

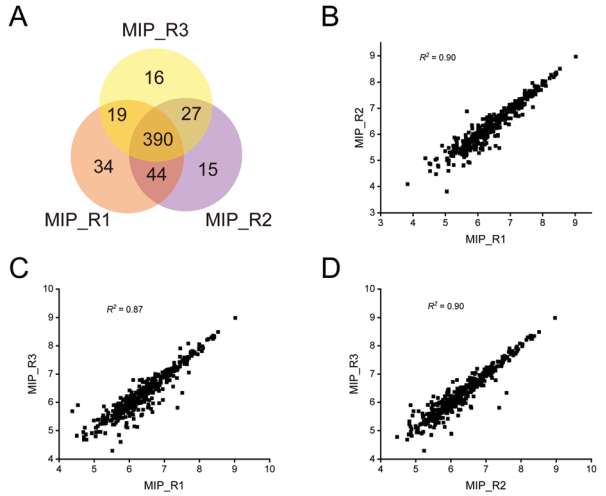

Fig. 6 The number and reproducibility of quantified exosome proteins from HeLa-CCM isolated by the MIP. (A) The Venn diagram of MIP-isolated exosome proteins quantified from the protein samples in triplicate. (B–D) The quantified reproducibility among three MS replicates.

their abundance was only 0.24%. The exclusion markers such as COX5B, PDAP1, HMGB2, SKP1, EIF4H, MAPRE1, PGM2, PTMA, HMGB3 and SLIRP were not identified.

To confirm that the proteins identified in the MIP-isolated exosomes from HeLa-CCM were *bona fide* exosome-associated proteins, we compared the proteomic data of our MIP-isolated exosomes with the human protein data annotated in the ExoCarta database, followed by GO analysis. As shown in Fig. 7D, 83.1% of the proteins in the MIP-isolated exosomes matched the human proteins annotated in the ExoCarta database. Protein–protein interaction (PPI) analysis of the subset of 451 proteins quantified in both MIP-isolated exosomes and the ExoCarta database revealed a highly interconnected network (Fig. S3B, ESI†). Prominent GO categories of the 451 proteins were related to extracellular exosomes, exhibited molecular functions such as cell adhesion molecule binding, protein binding and RNA binding, and participated in biological processes such as establishment of localization and transport (Fig. 7E). The above results indicate that the MIP can efficiently enrich exosomes from CCM. Prominent GO categories of the 92 proteins identified in MIP-isolated exosomes but not in the ExoCarta database were located in the extracellular region, Golgi apparatus, and extracellular space. These proteins participated in biological processes such as extracellular matrix organization and cellular responses to the vascular endothelial growth factor stimulus (Table S1, ESI†). It is more likely that these 92 proteins are derived from the Golgi apparatus.

To investigate the differences in exosome proteins between the urine and HeLa-CCM samples, we compared the proteins

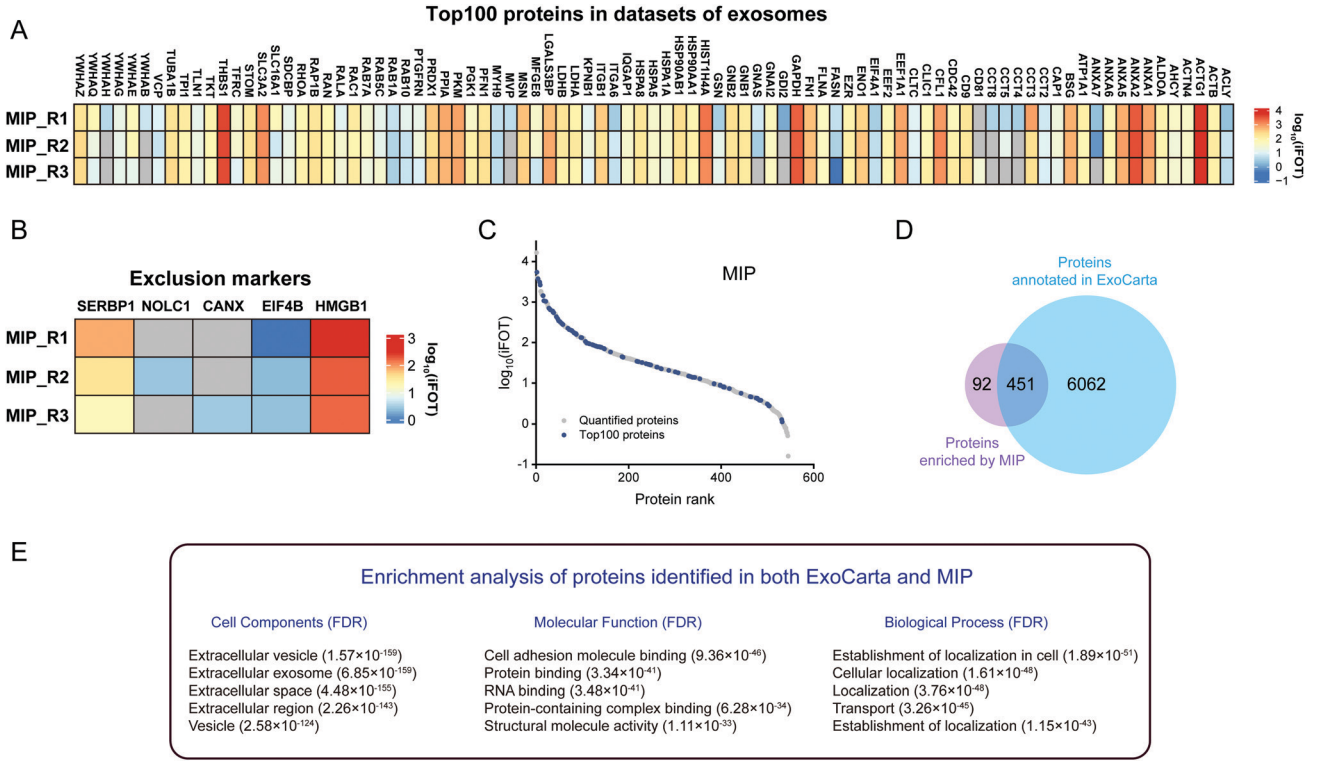

Fig. 7 Enrichment effect analysis of MIP-isolated HeLa-CCM exosomes based on the datasets of extracellular vesicles. (A) Heatmap of Top100 protein intensities in MIP-isolated exosomes. (B) Heatmap of exosomal exclusion marker intensities in MIP-isolated HeLa-CCM exosomes. (C) Ranking of quantified MIP-isolated HeLa-CCM exosome proteins based on iBAQ intensities. The Top100 proteins are marked in blue. (D) The Venn diagram of exosome proteins isolated by the MIP compared with proteins annotated in ExoCarta. (E) GO enrichment analysis for the cell components (left), molecular functions (middle) and biological processes (right) of proteins identified in both ExoCarta and the MIP.

identified in both ExoCarta and the MIP from the two samples. As shown in Fig. S4A (ESI†), 252 proteins were identified in both the urine and HeLa-CCM. These proteins perform binding functions such as cell adhesion molecule binding, protein binding and cadherin binding, and participate in biological processes such as regulated exocytosis, export from cells and secretion by cells (Fig. S4B, ESI†). These proteins reflected the basic characteristics of exosomes as cellular secretion, which may be ubiquitous in different samples. In contrast, the 879 exosome proteins uniquely identified in urine mainly perform functions such hydrolase activity and catalytic activity (Fig. S4C, ESI†). The 199 exosome proteins uniquely identified in the HeLa-CCM mainly perform functions such as RNA binding and structural molecule activity (Fig. S4C, ESI†). These differential proteins reflect the specificity of exosomes in different samples.

Conclusions

In summary, we put forward a simple method for the preparation of an artificial antibody for exosome capture by dull template imprinting technology. Due to the synergistic effect of topographical matching featured by molecular imprinting and the electrostatic interaction between the MIP and exosome membranes, the MIP had high capture efficiency and selectivity for exosomes in urine and cell culture media without the assistance of antibodies. Additionally, exosomes isolated from the MIP can be used for proteome analysis. Thus, the MIP holds promise in the exosome isolation and characterization fields.

Conflicts of interest

There are no conflicts to declare.

Acknowledgements

The authors are grateful for the financial support from the National Key R&D Programme of China (2017YFA0505003), the National Natural Science Foundation (21725506, 21775149, 22004012 and 21874131), the Doctoral Research Start-up Fund Project of Liaoning Province (2020-BS-190), the Talent innovation support program of Dalian (2019CT07), and the Innovation Fund Project of Dalian Institute of Chemical Physics (DICP I202030). K. Y. is an excellent member of the Youth Innovation Promotion Association, CAS (Y2021058), and China Postdoctoral Science Foundation (2020M670804).

References

1 R. Kalluri and V. S. LeBleu, *Science*, 2020, **367**, eaau6977.
2 G. van Niel, G. D'Angelo and G. Raposo, *Nat. Rev. Mol. Cell Biol.*, 2018, **19**, 213–228.
3 M. Mathieu, L. Martin-Jaular, G. Lavieu and C. Théry, *Nat. Cell Biol.*, 2019, **21**, 9–17.
4 G. Rodrigues, A. Hoshino, C. M. Kenific, I. R. Matei, L. Steiner, D. Freitas, H. S. Kim, P. R. Oxley, I. Scandariato, I. Casanova-Salas, J. Dai, C. R. Badwe, B. Gril, M. Tešić Mark, B. D. Dill, H. Molina, H. Zhang, A. Benito-Martin, L. Bojmar, Y. Ararso, K. Offer, Q. LaPlant, W. Buehring, H. Wang, X. Jiang, T. M. Lu, Y. Liu, J. K. Sabari, S. J. Shin, N. Narula, P. S. Ginter, V. K. Rajasekhar, J. H. Healey, E. Meylan, B. Costa-Silva, S. E. Wang, S. Rafii, N. K. Altorki, C. M. Rudin, D. R. Jones, P. S. Steeg, H. Peinado, C. M. Ghajar, J. Bromberg, M. de Sousa, D. Pisapia and D. Lyden, *Nat. Cell Biol.*, 2019, **21**, 1403–1412.
5 C. Liu, J. Zhao, F. Tian, L. Cai, W. Zhang, Q. Feng, J. Chang, F. Wan, Y. Yang, B. Dai, Y. Cong, B. Ding, J. Sun and W. Tan, *Nat. Biomed. Eng.*, 2019, **3**, 183–193.
6 J. Jiang, J. Mei, Y. Ma, S. Jiang, J. Zhang, S. Yi, C. Feng, Y. Liu and Y. Liu, *Exploration*, 2022, **2**, 20210144.
7 N. Karimi, A. Cvjetkovic, S. C. Jang, R. Crescitelli, M. A. Hosseinpour Feizi, R. Nieuwland, J. Lötvall and C. Lässer, *Cell. Mol. Life Sci.*, 2018, **75**, 2873–2886.
8 Y. Tian, M. Gong, Y. Hu, H. Liu, W. Zhang, M. Zhang, X. Hu, D. Aubert, S. Zhu, L. Wu and X. Yan, *J. Extracell. Vesicles*, 2019, **9**, 1697028.
9 J. Webber and A. Clayton, *J. Extracell. Vesicles*, 2013, **2**, 19861.
10 F. A.-W. Coumans, A. R. Brisson, E. I. Buzas, F. Dignat-George, E. E.-E. Drees, S. El-Andaloussi, C. Emanueli, A. Gasecka, A. Hendrix, A. F. Hill, R. Lacroix, Y. Lee, T. G. van Leeuwen, N. Mackman, I. Mäger, J. P. Nolan, E. van der Pol, D. M. Pegtel, S. Sahoo, P. R.-M. Siljander, G. Sturk, O. de Wever and R. Nieuwland, *Circ. Res.*, 2017, **120**, 1632–1648.
11 A. Kumar, S. R. Dhadi, N. N. Mai, C. Taylor, J. W. Roy, D. A. Barnett, S. M. Lewis, A. Ghosh and R. J. Ouellette, *J. Extracell. Vesicles*, 2021, **10**, e12138.
12 T. Takeuchi, K. Mori, H. Sunayama, E. Takano, Y. Kitayama, T. Shimizu, Y. Hirose, S. Inubushi, R. Sasaki and H. Tanino, *J. Am. Chem. Soc.*, 2020, **142**, 6617–6624.
13 G. Li, N. Zhu, J. Zhou, K. Kang, X. Zhou, B. Ying, Q. Yi and Y. Wu, *J. Mater. Chem. B*, 2021, **9**, 2709–2716.
14 N. Zhu, G. Li, J. Zhou, Y. Zhang, K. Kang, B. Ying, Q. Yi and Y. Wu, *J. Mater. Chem. B*, 2021, **9**, 2483–2493.
15 C. Gardiner, D. D. Vizio, S. Sahoo, C. Théry, K. W. Witwer, M. Wauben and A. F. Hill, *J. Extracell. Vesicles*, 2016, **5**, 32945.
16 M. Ding, C. Wang, X. Lu, C. Zhang, Z. Zhou, X. Chen, C.-Y. Zhang, K. Zen and C. Zhang, *Anal. Bioanal. Chem.*, 2018, **410**, 3805–3814.
17 N. Zhang, N. Sun and C. Deng, *Talanta*, 2021, **221**, 121571.
18 Y. Wan, G. Cheng, X. Liu, S.-J. Hao, M. Nisic, C.-D. Zhu, Y.-Q. Xia, W.-Q. Li, Z.-G. Wang, W.-L. Zhang, S. J. Rice, A. Sebastian, I. Albert, C. P. Belani and S.-Y. Zheng, *Nat. Biomed. Eng.*, 2017, **1**, 0058.
19 A. Kumar, S. R. Dhadi, N. N. Mai, C. Taylor, J. W. Roy, D. A. Barnett, S. M. Lewis, A. Ghosh and R. J. Ouellette, *J. Extracell. Vesicles*, 2021, **10**, e12138.
20 L. Liu, C. Dong, X. Li, S. Li, B. Ma, B. Zhao, X. Li, Z. Liang, K. Yang, L. Zhang and Y. Zhang, *Small*, 2020, **16**, 1904199.
21 L. Liu, K. Yang, H. Gao, X. Li, Y. Chen, L. Zhang, X. Peng and Y. Zhang, *Anal. Chem.*, 2019, **91**, 2591–2594.
22 L. Liu, K. Yang, Z. Dai, Z. Liang, L. Zhang, X. Peng and Y. Zhang, *Chin. Chem. Lett.*, 2019, **30**, 672–675.

23 N. Heath, L. Grant, T. M. De Oliveira, R. Rowlinson, X. Osteikoetxea, N. Dekker and R. Overman, *Sci. Rep.*, 2018, **8**, 5730.
24 X. Li, C. Zhang, T. Gong, X. Ni, J. E. Li, D. Zhan, M. Liu, L. Song, C. Ding, J. Xu, B. Zhen, Y. Wang and J. Qin, *Nat. Commun.*, 2018, **9**, 4910.
25 H. Malhotra, N. Sheokand, S. Kumar, A. S. Chauhan, M. Kumar, P. Jakhar, V. M. Boradia, C. I. Raje and M. Raje, *J. Biomed. Nanotechnol.*, 2016, **12**, 1101–1114.
26 F. G. Kugeratski, K. Hodge, S. Lilla, K. M. McAndrews, X. Zhou, R. F. Hwang, S. Zanivan and R. Kalluri, *Nat. Cell Biol.*, 2021, **23**, 631–641.
27 S. Mathivanan, C. J. Fahner, G. E. Reid and R. J. Simpson, *Nucleic Acids Res.*, 2011, **40**, D1241–D1244.
28 M. Pathan, P. Fonseka, S. V. Chitti, T. Kang, R. Sanwlani, J. Van Deun, A. Hendrix and S. Mathivanan, *Nucleic Acids Res.*, 2019, **47**, D516–D519.